

- 1
- 2
- 3
- 4
- 5
- 6
- 7
- 8
- 9
- 10
- 11
- 12
- 13
- 14
- 15
- 16
- 17
- 18
- 19

4
56
7

8
9
10

11
1213
14

15

16

17
18

19



Abstract

This study examined how the addition of modified cornstalk biochar (CB) affected ammonia (NH₃) emissions during composting. Four treatments were established, including a control (CK) with layer manure and sawdust only, and the CK mixtures adding 10% HNO₃ CB (NA), 10% H₂O₂ CB (HP) and 10% HNO₃- H₂O₂ CB (MI). As the results showed, NH₃ emissions was reduced by 47.83% (NA), 61.69% (HP) and 45.69% (MI) when the modified CB used as a compost additive ($P < 0.05$). According to the data analysis, the addition of modified CB significantly increased the number of ammonia-oxidizing bacteria (AOB), inhibited urease activity and decreased the abundance of *narG* and *nirS* at rising temperatures and high temperatures ($P < 0.05$). Redundancy analysis demonstrated a negative correlation between NH₃ emissions and AOB and a positive correlation with urease activity, *narG* and *nirS*. Thus, the modified CB helped reduce NH₃ emissions by regulating nitrification processes.

Keywords: Composting, Layer manure, Biochar, Ammonia, Nitrogen functional gene

1. Introduction

China's laying hen industry has long been ranked first in the world in terms of its breeding scale and egg production, and the annual demand for commercial laying hens has remained between 1.3-1.5 billion. However, the resulting large amount of laying hen manure (LM) contains a large amount of pollutants, including suspended solids, salt, gas, bacteria and viruses; if directly discharged without proper disposal, this material will seriously pollute the surrounding air, water and soil (Wang et al., 2020). Therefore, how to quickly and effectively deal with LM has become an important issue in the industry, restricting its sustainable development.

Composting is well-known as a transformation process from manure into reliable and stable final products served as substrates and nutrients for plant growth (Akdeniz, 2019; Tsui et al., 2019). The discharge of various harmful gases during the composting process has impeded the development of these practices (Rincon et al., 2019). Ammonia (NH₃) emissions are a problem that cannot be ignored. NH₃ volatilization is the major way of nitrogen loss from compost (Guo et al., 2020a). Prior studies have demonstrated that approximately 9.6%–46% of the initial total nitrogen (TN) is lost in the form of NH₃, taking up 79%–94% of the TN loss during composting (de Guardia et al., 2008). During the temperature increase and high temperature stages of composting, microorganisms decompose organic nitrogen compounds through ammonization to produce NH₃ (Chen et al., 2020a). Urease is the key enzyme catalyzing the decomposition of carbamide into NH₃ and carbonic acid (Meng et al., 2020). NH₃ dissolves

in water to form ammonium nitrogen ($\text{NH}_4^+\text{-N}$), and $\text{NH}_4^+\text{-N}$ accumulates rapidly and increases the pH value of the reactor. As the temperature and pH of compost rising, the conversion process of nonvolatile $\text{NH}_4^+\text{-N}$ to volatile NH_3 in the material is intensified, and NH_3 volatilization becomes particularly intense (Wu et al., 2020; Yu et al., 2020). The composition process of converting $\text{NH}_4^+\text{-N}$ into nitrate nitrogen ($\text{NO}_3^-\text{-N}$) and fixing in the compost requires nitrifying bacteria, which is mainly controlled by ammonia-oxidizing bacteria (AOB) (Chen et al., 2020b; Wu et al., 2020). Nitrifying bacteria are medium-temperature bacteria that cannot endure high temperatures. Therefore, without bacterial activity, $\text{NH}_4^+\text{-N}$ cannot be converted into $\text{NO}_3^-\text{-N}$. After the compost enters the cooling and decay stage, the temperature continues to decrease, nitrification is enhanced, ammonium nitrogen continues to decrease, $\text{NO}_3^-\text{-N}$ concentration increases, and NH_3 volatilization decreases (Ren et al., 2020; Zhang et al., 2020b). Four nitrogen functional genes, namely, *narG*, *nirK*, *nirS* and *nosZ*, have generally been applied to characterize nitrogen-fixing and denitrifying communities. The *narG* genes catalyze the conversion of $\text{NO}_3^-\text{-N}$ to $\text{NO}_2^-\text{-N}$. The *nirK* and *nirS* genes are the key genes for converting $\text{NO}_2^-\text{-N}$ to NO. The reduction of N_2O to N_2 is catalyzed by *nosZ* and is the final reaction step in the denitrification pathway (Yu et al., 2020; Zhang et al., 2020a).

The methods currently used for NH_3 emissions reduction during composting mainly include the addition of different microorganisms and bulking agents (Awasthi et al., 2020; Li et al., 2020) and the adjustment of composting conditions (Akiyama et al., 2020). Among those, the employment of bulking agents is considered an effective way to decrease the amount of NH_3 emissions (Chen et al., 2017; Guo et al., 2020b). The physiochemical properties of biochar vary in terms of different feedstocks used, including surface charge and specific surface areas (Sohi, 2020). Previous studies by our team showed that adding 10% bamboo biochar, cornstalk biochar, coir biochar, woody biochar and layer manure biochar to compost could reduce NH_3 emissions by 22.70%, 33.11%, 21.51%, 32.87% and 24.19%, respectively (Chen et al., 2017). Adding cornstalk biochar to compost has NH_3 emissions reducing effects. Recent evidence suggests that the addition of biochar can reduce NH_3 emissions released during composting by 6.35%-36.20% (He et al., 2019; Liu et al., 2017; Liu et al., 2020). However, the current emission reduction efficiency is not high enough, and hence we hope to continue to improve the effect of ammonia emission reduction. HNO_3 and H_2O_2 are commonly used biochar modification oxidants. Through the corresponding surface chemical modifications of various biochar, the adsorption performance of biochar can be improved (Zhu et al., 2020). Furthermore, the increase in the pore

structure of modified biochar can increase its adsorption capacity (Liang et al., 2017); however, to date, no research has surveyed the use of modified biochar to reduce the emission of NH_3 in compost. It is highly feasible that the adsorption capacity of biochar can be increased through surface oxidation and that this material can further reduce harmful gas emissions from composting.

In conclusion, this research intends to unravel the effects of biochar modification in different ways on the physical-chemical properties of compost and NH_3 emissions and to explicate the mechanisms probably involved. Hopefully, this paper sheds new light on a new method of decreasing NH_3 emissions during the LM composting process.

2. Materials and methods

2.1. Composting mixtures

The materials of composting comprise layer manure (LM), sawdust (SW) and cornstalk biochar (CB), which were used as compost additives. The LM that we made use of was assembled from a chicken farm situated at the Experiment Station and Agriculture Training Center, South China Agricultural University, Guangzhou, China. The SW (2 mm mesh size) residue was collected from the Zengcheng District, Guangzhou, China, which is used to regulate the C/N ratio and moisture content of the compost. CB was acquired from the Henan Zhongbiao Environmental Protection Technology Co., Ltd. located in Zhengzhou. Twelve 19 L laboratory simulators for composting were used in the study, each of which was loaded with fresh LM (6.0 kg), SW (2.0 kg, which was 30% by wet weight (w/w) of the LM). The key physicochemical characteristics of LM, SW and BC are demonstrated in Table 1 and Table 2.

2.2. Modified CB preparation

First, the CB was immersed in deionized water for 24 h and then repeatedly washed until the water quality was clear to remove the impurities attached to the surface of the biochar. Then, the cleaned CB was placed in a stove and baked at 105 °C for 24 h. After being removed, it was cooled to room temperature and sealed for use.

2.2.1 HNO_3 modification

1.6 kg of the above-mentioned CB was placed in a conical flask with a stopper, with 16 L of a 6 mol/L HNO_3 solution added and then shook with an oscillator for 6 h at a 26-degree constant temperature. After shaking, the mixture was filtered and then repeatedly washed with a large amount of deionized water until the filtrate was close to neutral to remove excess HNO_3 solution. The cleaned CB was placed into the stove and dried at 105 °C for 24 h. After cooling, it was sealed and

used for preparation (Li et al., 2014; Lin et al., 2012).

2.2.2 H₂O₂ modification

0.8 kg of the above-mentioned CB was placed in another conical flask, with 8 L of a 25% H₂O₂ solution added and then shook in the same condition as above. After shaking, the mixture was filtered and then repeatedly washed with a large amount of deionized water until the filtrate was close to neutral to remove excess H₂O₂ solution. The cleaned CB was placed into the stove and dried at 105 °C for 24 h as well. After cooling, it was sealed and used for preparation (Huff & Lee, 2016; Xue et al., 2012).

2.2.3 HNO₃ and H₂O₂ mixed modification

A total of 0.8 kg of 6 mol/L HNO₃-modified CB was placed in a conical flask, and 8 L of a 25% H₂O₂ solution was added and then shaken with other conditions being equal. Then, the mixture was filtered, and the solution was repeatedly washed with a large amount of deionized water until the filtrate was close to neutral to remove excess H₂O₂ solution. The cleaned CB was placed into the stove and dried at 105 °C for 24 h. After cooling, it was sealed and used for preparation.

2.3. Experimental design

The experiment was divided into four treatments. The mixture of LM and SW only (that is, without any CB) was treated as a control (CK), with different types of modified CB (0.80 kg, which was 10% by w/w of the LM and SW) added to the CK being other three treatments. The treatments were labeled NA (for HNO₃-modified CB), HP (for H₂O₂-modified CB), and MI (for HNO₃ and H₂O₂ mixed-modified CB). All repeats three times per group. The initial moisture content of the composting mixtures was regulated to between 50% and 55%. Throughout the composting process, fresh air (0.2 m³·h⁻¹·kg⁻¹) was constantly pumped into the compost by a whirlpool pump and a gas flowmeter. The temperature of each compost was measured and recorded with a mercury thermometer c daily at 09:00, 16:00 and 22:00. When the pile temperature dropped to ambient temperature, the composting stopped after 12 days.

2.4. Sample collection

The compost samples were collected on days 0, 1, 3, 5, 8, and 12. Each compost had an automatic turnover device to make it even, and -was flipped for 3 min before sampling each day. The samples were stored at -80 °C. The approaches of NH₃ collection were performed similarly as previous studies (Chen et al., 2017; Zhou et al., 2019).

2.5. Analytical methods

2.5.1 Gaseous measurements and physicochemical analyses

To evaluate the daily NH_3 emission during the composting, the ammonia was absorbed in dilute sulphuric acid (0.5 mol/L, 300 ml) for 24 h and concentration was determined according to Nessler's Reagents spectrophotometer (Chen et al., 2017; Zhou et al., 2019). Urease activity was measured using a Soli-Urease, S-UE kit (Solid- Urease, S- UE, Nanjing Jiancheng Bioengineering Institute). The specific surface area and the total pore volume of pristine and modified biochar were measured by a Brunauer-Emmett-Teller analyzer (BET, Micromeritics ASAP 2460, USA) using N_2 adsorption-desorption method.

2.5.2 Molecular microbiology analysis

Genomic DNA was extracted adopting the Soil DNA Kit (Omega Bio-Tek, Inc.). The extracted DNA samples were gathered and stored immediately at -20°C until analysis. The qPCR method was applied to examine nitrogen functional genes, including AOB-*amoA*, *narG*, *nirS*, *nirK*, and *nosZ*. Table 3 lists the sequence and annealing temperature of specific primers. qPCR was performed on a Bio-Rad CFX96 PCR System. All gene samples were subjected to 1% agarose gel electrophoresis, and was recovered by the gel extraction kit (OMEGA). The specific steps of qPCR referred to previous research (Zhou et al., 2019)

2.6. Statistical analysis

The data were statistically collected and analyzed by one-way analyses of variance (ANOVAs) by SPSS (SPSS v. 17.0), presented as the average value (standard deviation). The observed variance with $P < 0.05$ was regarded statistically significant. The redundancy analysis (RDA) revealed the relationship among all parameters analyzed (R Studio v. 1.14).

3. Results and discussion

3.1. Ammonia emissions

~~The total NH_3 emissions of CK, NA, HP and MI were 5986.38 ± 122.02 , 3122.85 ± 94.20 , 2293.28 ± 119.31 and 3251.24 ± 88.28 mg, respectively (Fig. 1(a)). Compared to the CK group, the NH_3 emissions of NA, HP and MI were reduced by 47.83%, 61.69% and 45.69%, respectively ($P < 0.05$), and the NH_3 emissions reduction rate of group HP was significantly higher than that of the other groups ($P < 0.05$). Thus, it can be seen that adding modified CB to compost can effectively reduce the NH_3 emissions, and the addition of H_2O_2 -modified biochar especially works the best in NH_3 emissions reduction.~~

As shown in Figure 1(b), in all groups, the amount of daily NH_3 emissions increased at first, then decreased and finally reached a plateau. The peak NH_3 emissions of groups CK (1621.85 ± 73.44 mg/d), NA (894.07 ± 26.37 mg/d) and MI (975.55 ± 110.17 mg/d) on day 2, and the peak NH_3 emissions of HP

(701.48 ± 53.13 mg/d) on day 3. Analysis of variance showed that the peak NH₃ emissions of NA, HP and MI were significantly lower than those of CK ($P < 0.05$). There was no significant difference in NH₃ emissions between the NA and HP groups during composting ($P > 0.05$), and the NH₃ emissions of the HP group were significantly lower than those of the other three groups ($P < 0.05$). Liu et al. (2020) reached a similar conclusion, reporting peak NH₃ emissions in the warming period, with low emissions during the cooling period.

The total NH₃ emissions of CK, NA, HP and MI were 5986.38 ± 122.02, 3122.85 ± 94.20, 2293.28 ± 119.31 and 3251.24 ± 88.28 mg, respectively. Compared to the CK group, the NH₃ emissions of NA, HP and MI were reduced by 47.83%, 61.69% and 45.69%, respectively ($P < 0.05$), and the NH₃ emissions reduction rate of group HP was significantly higher than that of the other groups ($P < 0.05$). Thus, it can be seen that adding modified CB to compost can effectively reduce the NH₃ emissions, and the addition of H₂O₂-modified biochar especially works the best in NH₃ emissions reduction.

3.2. Changes in physicochemical factors during composing

As shown in Figure 2, there was basically no significant difference in the physical chemical indicators between groups, indicating that the addition of modified CB would not affect the composting process.

Moisture is a key factor supporting the growth and reproduction of microorganisms, which plays a vital role in decomposing organic matter, thus further affecting the composting process (Thomas et al., 2020). The changes, as shown in Fig. 2(a), showed a slight decrease, which could be explained by the loss of vapor in the process of water evaporation. The initial moisture contents of CK, NA, HP and MI were 54.56 ± 0.55%, 52.83 ± 0.77%, 53.76 ± 0.24% and 53.10 ± 0.38%, respectively. The moisture of the HP group was evidently higher than that of the other groups on day 12 ($P < 0.05$). Higher moisture could dissolve more NH₃.

The temperature changes in the tests of each group and the ambient variation are shown in Fig. 2(b). During the entire composting process, the vessels were heated and then cooled down. Similar regularity was found in the different treatments, with the temperature reaching its peak maintaining for near five days and gradually cooling. Starting from the eighth day, the temperature of each group began to decrease. The highest temperatures of the compost in CK, NA, HP and MI were 50.67 ± 0.33, 49.67 ± 0.67, 48.67 ± 0.33 and 49.67 ± 0.65 °C, respectively. The temperature of each group dropped rapidly on the eighth day because the auxiliary heating equipment was turned off. The variance analysis revealed that

throughout the composting process, there was no significant variance observed in temperature between groups ($P > 0.05$).

pH is another influential factor for microbial biological activity and community structure during composting. The trends of changing in pH followed a similar regularity between groups (Fig. 2(c)), that is, increasing rapidly and then leveling off to a constant value. During composting, no significant difference was founded in the pH of CK (7.06 - 8.30), NA (7.24 - 8.20), HP (6.65 - 8.20) and MI (6.64 - 8.13) ($P > 0.05$). The composting materials were slightly alkaline (pH 8.00-9.00) on day 12. The dissolution of NH_3 and the decomposition of organic acids accounted for the increase in pH values (Gajalakshmi & Abbasi, 2008; Liu et al., 2011).

The measurements of electrical conductance (EC) are able to reflect the variance of soluble salts in the composting process, and the higher the conductivity, the higher the soluble salt content (Huang et al., 2004). The EC values were 2.41- 2.83 mS/cm at first and decreased over time to 1.40 - 2.38 mS/cm on day 12 (Fig. 2(d)). Several primary factors could contribute to these phenomena, such as the volatilization of NH_3 and humification, where all types of small molecule organic acids and salts will be fixed and macromolecules will be transformed into humus (Liang et al., 2006). The EC of the treatment groups with 10% biochar added was significantly higher than that of the CK on day 12. The significantly increasing conductivity of the compost after adding biochar may be ascribed to the relatively high conductivity of the biochar itself. Zhang et al. (2014) reached a similar conclusion that a large quantity of surface negative charges and the high cation exchange capacity of biochar could have accounted for such increase in EC as well.

As shown in Figure 2 (e), the values of C/N are an important indicator to assess whether the compost has been completely plateauing (Chen et al., 2020c). When the C/N values of the compost are too high, the relatively excessive amount of carbon and relatively lack of nitrogen will hinder the growth of microorganisms and thus slow down the composting process. When the C/N values of the compost are too low, it might cause the conversion of nitrogen into NH_3 gas, which would volatilize, thus leading to nitrogen loss (Akiyama et al., 2020). Changes in the C/N values were basically identical between groups, with all rising at the early stage and then plateauing. The initial C/N values of CK, NA, HP and MI were 13.17 ± 0.41 , 16.87 ± 1.31 , 15.75 ± 1.08 , 15.22 ± 1.36 and 15.25 ± 1.88 , respectively. The C/N values of CK, NA, HP and M were 32.49 ± 3.26 , 38.63 ± 2.77 , 39.79 ± 1.76 , 36.29 ± 1.25 , respectively, on day 12.

No significant difference in C/N was founded between groups, which further suggested that the addition of modified CB made no significant difference to the C/N values and composting progress.

Total organic carbon (TOC) are responsible for the carbon source for microbial aerobic fermentation. During the composting process, TOC continuously degrades, providing energy for microorganisms and enabling them to grow and reproduce rapidly. TOC undergoes a complicated process to form humus, thereby increasing the fertility of the compost (Zhao et al., 2020). The variation in TOC during composting is shown in Fig. 2(f). Changes in the TOC concentrations were not significantly different in each group during composting ($P > 0.05$). The initial TOC concentrations of CK, NA, HP and MI were 399.80 ± 8.55 , 412.53 ± 11.56 , 416.00 ± 4.93 and 415.10 ± 8.72 g/kg, respectively. The TOC values of CK, NA, HP and MI were 429.03 ± 9.16 , 401.82 ± 4.07 , 394.28 ± 8.73 and 408.37 ± 11.21 g/kg, respectively, on day 12. Furthermore, the analysis revealed that the addition of BC resulted in enhancement of the decomposition of TOC. Malińska et al. (2014) came to a similar conclusion.

3.3. Nitrogen conversion and changes in urease activity

Nitrogen is necessary for the microbial fermentation of nutrients, especially for protein synthesis and energy. In the process of composting, organic nitrogen produces NH_3 through amination, and part of the NH_3 dissolves into the heap to produce $\text{NH}_4^+\text{-N}$. Nitrification stands for the biological conversion of ammonium nitrogen ($\text{NH}_4^+\text{-N}$) to nitrite nitrogen ($\text{NO}_3^-\text{-N}$) (Yu et al., 2020). As Figure 3(a) illustrates, the TN trend of each group was basically the same, showing a trend of gradually decreasing and then plateauing. At the starting point of composting, the TN concentration of all groups increased to their peak, with the highest values in CK, NA, HP and MI being 26.47 ± 0.76 g/kg, 24.66 ± 1.36 g/kg, 30.73 ± 0.59 g/kg and 27.38 ± 1.09 g/kg, respectively. At the ending phase of composting, the TN contents in CK, NA, HP and MI were 9.93 ± 0.31 g/kg, 10.43 ± 0.36 g/kg, 13.52 ± 1.60 g/kg and 11.28 ± 0.66 g/kg, respectively. The HP group had a significantly higher TN concentration than the CK group ($P < 0.05$). In other words, the H_2O_2 -modified biochar exerted a certain impact on nitrogen fixation as the temperature rose. The TN loss rates of CK, NA, HP and MI were 62%, 57%, 56% and 58%, respectively.

As Figure 3(b) illustrates, the regularity of $\text{NH}_4^+\text{-N}$ was basically identical in each group, with a trend rising first and then falling. After reaching the maximum levels, the amount of $\text{NH}_4^+\text{-N}$ subsequently decreased and then plateauing by the end of the composting owing to NH_3 volatilization and nitrification. There was no marked difference between the different groups ($P > 0.05$). Broadly speaking, the $\text{NO}_3^-\text{-N}$ concentration of all groups increased in the initial and final stages of composting. As shown in Figure

3(c), the average NO_3^- -N concentrations in CK, NA, HP and MI were 0.35 ± 0.03 , 0.42 ± 0.03 , 0.45 ± 0.03 and 0.39 ± 0.02 g/kg, respectively. By contrasting the changing trend, the NO_3^- -N concentration was found to be significantly higher in HP than in CK ($P < 0.05$) during the entire process, and it was evidently higher in NA than in CK on days 3, 8 and 12 ($P < 0.05$). The NO_3^- -N concentration was significantly higher in MI than in CK on days 1, 5, 8 and 12 ($P < 0.05$). The above analysis showed that the modified biochar could prompt the process of composting, especially through nitrification in the rising- and high-temperature stages, increasing the concentration of NO_3^- -N.

Urease is known as the major enzyme catalyzing the decomposition of carbamide into NH_3 and carbonic acid (Meng et al., 2020). According to Figure 3(d), the variation trend of urease activity in each group was basically the same, with an upward tendency and then decreasing. On days 1 and 3, the urease activity in the NA, HP and MI groups was markedly higher than that in the CK group ($P < 0.05$). The peak urease activity of each group occurred on day 1, and the urease activity in each group was 2582.65 ± 112.52 , 2118.14 ± 221.08 , 1949.63 ± 59.88 and 2048.78 ± 119.85 U/g. After the urease activity increased, it could catalyze the decomposition of carbamide to produce NH_3 , so the peak NH_3 emissions in each group were on day 2 or 3. As the composting progressed, the urease activity of each group gradually decreased, and NH_3 emissions gradually decreased.

3.4. The changes in the abundances of total bacteria, ammonia-oxidizing bacteria and four kinds of genes during the composting process

The variation in the absolute abundance of total bacteria in each group is illustrated in Figure 4(a). During the entire composting process, the changes in the total bacterial counts of each group were basically identical, with a rapid increase and then a rapid decrease before a slight increase at the end. Two days before composting, the temperature had risen slowly, which provides suitable conditions for the growth and reproduction of bacteria. As a result, the total count increased. By day 1, as the temperature rose, most of the heat-intolerant bacteria were inhibited, leading to a decrease in their total numbers and an increase in the activity of thermophilic bacteria. At this time, the number of bacteria in each group reached its peak, and the log values of their copy numbers in each group were 10.69 ± 0.016 , 11.04 ± 0.035 , 11.20 ± 0.028 and 10.73 ± 0.033 , respectively. After cooling began, the major thermophilic bacteria were recovered and reproduced. In this manner, the total number of bacteria increased. By day 8, the numbers of bacteria in each group reached the lowest levels, and the log values of their copy numbers in each group were 9.86 ± 0.011 , 10.25 ± 0.027 , 10.49 ± 0.031 and 10.21 ± 0.015 , respectively.

The number of total bacteria in the HP and NA groups was notably higher than that in the CK group ($P < 0.05$) throughout the composting. The total bacterial count in the MI group was higher than that in the CK group on days 3, 5, 8 and 12 ($P < 0.05$). Therefore, the addition of modified biochar can increase the number of microorganisms in compost. Adding the different types of modified biochar increased the total bacteria population in the compost, which might have benefited from their immense specific superficial area and pore structure, providing a good environment for the attachment and reproduction of microorganisms (Tsui et al., 2018; Wei et al., 2014).

Ammonia oxidation is believed to be a crucial and rate-limiting step in the composting process and is catalyzed by the ammonia monooxygenase (AOB *amoA* genes) produced by AOB (Awasthi et al., 2018). The changing trend in the absolute abundance of AOB in each group is illustrated in Figure 4 (b). During the whole composting process, the abundance of AOB in each group tended to be identical, rapidly increasing and then rapidly decreasing and slightly increasing in the final stage. The change trend of AOB and total bacteria population was basically the same. Throughout the composting, the log values of the copy numbers of AOB in each group were between 5.27 and 5.84. By day 1, the amount of AOB in each group peaked, and the log values of the copy numbers of AOB in each group were 5.69 ± 0.018 , 5.82 ± 0.025 , 5.84 ± 0.026 and 5.76 ± 0.039 , respectively. By day 8, the numbers of AOB in each group reached the lowest levels, and the log values of the copy numbers of AOB in each group were 5.29 ± 0.009 , 5.38 ± 0.016 , 5.39 ± 0.041 and 5.34 ± 0.022 , respectively. The number of AOB in the HP and NA groups was significantly higher than that in the CK group ($P < 0.05$) during the entire composting process. The number of AOB in the MI group was significantly higher than that in the CK group on days 1, 3 5 and 8 ($P < 0.05$). Nitrifying bacteria, as aerobic microorganisms, are likely to benefit from cornstalk biochar for providing a favorable microenvironment and enhancing aerobic conditions and increasing colonization, thus enhancing the nitrification process (López-Cano et al., 2016; Sánchez-García et al., 2015). Since AOB is capable of promoting the transformation from ammonium nitrogen to nitrate nitrogen, the mechanism by which modified biochar reduces NH_3 emissions may be via the promotion of the transformation from $\text{NH}_4^+\text{-N}$ to $\text{NO}_3^-\text{-N}$ (Wu et al., 2020).

The abundances of denitrifying genes such as *narG* (Fig. 4(c)), *nirK* (Fig. 4(d)), *nirS* (Fig. 4(e)) and *nosZ* (Fig. 4(f)) under the different treatments are given in Figure 4. The *narG* gene was responsible for facilitating the first step of denitrification, that is, NO_2^- production from the reduction of NO_3^- . Both *nirK* and *nirS* genes are needed in the conversion of NO_2^- into NO. The *nosZ* gene functions in

converting N₂O into N₂ (Zhang et al., 2015). As composting progresses, the abundance of denitrification genes varies among groups, but compared with the beginning of composting, the abundance of denitrification genes in each group increased. In the prior stage of composting, no significant difference in denitrification genes was noticed among the groups ($P > 0.05$). At the end of composting, the addition of biochar to the compost significantly increased the abundance of the *narG*, *nirK* and *nosZ* genes ($P < 0.05$). According to Li et al. (2016), the abundance of *narG* changed dramatically with the compost being added to the soil. The application of biochar played a prominent role in *nirK* and *nosZ* but exerted a limited impact on *nirS*. The changes in the abundance of the *nosZ* gene could be ascribed to the changes in pH because biochar as an electron shuttle or donor will induce anoxic microsite formation (Yu et al., 2020). Prior studies have shown that relatively high abundance of *nosZ* gene could reduce N₂O emissions in compost. Adding modified biochar can promote the denitrification reaction, thereby reducing NH₃ emissions.

3.5. The relationship between environmental parameters and genes

During composting, several physicochemical factors had affected the cycle of nitrogen, including temperature, pH, moisture, TOC and nitrogen transformation (NH₄⁺-N, NO₃⁻-N, TN and NH₃), which were examined with RDA to identify the correlation between physicochemical factors and denitrification genes during composting. Redundancy analysis (RDA) was used to compare the correlation between NH₃ and nitrogen functional genes and physicochemical indicators among all treatments (Fig. 5). As seen from the figures, although a slightly stronger relationship between each factor was observed for the biochar treatments than that without modified biochar application, the correlations observed in the four treatment groups were extremely similar. As shown in the RDA, NH₃ emissions were positively correlated with pH, temperature, C/N, *narG*, *nirK*, *nosZ*, and *nirS*, and among them, the pH, temperature and C/N had the greatest influence on NH₃ emissions in each group. Liu et al. (2019) reached a similar conclusion. The figure shows that NH₃ emissions were negatively correlated with moisture, TN, total bacteria and AOB. The moisture of the HP group was notably higher than that of the other groups on day 12 ($P < 0.05$). And the HP group had a significantly higher TN concentration than the CK group ($P < 0.05$). The numbers of total bacteria and AOB in the NA, HP and MI groups were significantly higher than those in the CK group on days 3, 5, 8 and 12 ($P < 0.05$). NH₃ emissions were inversely related to moisture, TN, total bacteria and AOB. Thus, one of the reasons for the low NH₃ emissions was the high moisture and the large number of total bacteria. By day 3, modified CB groups decreased the abundance

of *narG* and *nirS*, and NH_3 emissions were positively correlated with *narG* and *nirS*. In the CK and HP groups, NH_3 was negatively correlated with urease activity, and high urease activity results in the production of more NH_3 . Therefore, the reasons for the low NH_3 emissions were the low abundance of *narG* and *nirS* and low urease activity.

3.6. The Brunauer-Emmett-Teller (BET) model results for the different treatments

The BET model results are illustrated in Table 4. Compared with the CK, the specific surface area of the NA, HP and MI groups increased by 56.30%, 90.14% and 58.72%, respectively. The total pore volume of the NA, HP and MI groups increased by 33.48%, 143.32% and 46.21% respectively, compared with that in the CK group. The BET model results indicated that compared to the other groups, the HP group had a larger specific surface area and total pore volume. Larger surface areas and pore sizes could absorb more NH_3 . The microscopic pore structure of the HP group connects the pores to each other, which facilitates gas absorption and aerobic reactions (Kazak et al., 2020). This may be one of the reasons why the HP group had the highest NH_3 emissions reduction rate.

4. Conclusion

The ~~present~~ study ~~indicated~~ showed that the additive oxidized modified biochar could significantly reduce NH_3 emissions by 47.83% (NA), 61.69% (HP) and 45.69% (MI) ($P < 0.05$), which ~~The results~~ indicated that adding modified CB could obviously improve the number of AOB, inhibit urease activity and decrease the abundance of *narG* and *nirS* ($P < 0.05$), ~~thus~~ Thus, facilitating the transformation of ~~ammonium-nitrogen~~ NH_4^+ -N into NO_3^- -N ~~nitrate-nitrogen~~ and decreasing nitrogen loss. Compared with those of ~~the CK-group~~, the specific surface area and total pore volume of ~~the~~ HP ~~group~~ increased by 90.14% and 143.32%, respectively. This study contributes to addressing odor issues associated with LM compost and hopefully could promote the technological development of composting industry.

CRedit authorship contribution statement

Shizheng Zhou: Conceptualization, Methodology, Investigation, Formal analysis, Writing - original draft, Writing - review & editing. **Ran Cheng** and **Yuliang Qian:** Investigation. **Xin Wen** and **Jiandui Mi:** Conceptualization, Writing - review & editing. **Zhen Cao, Yan Wang, Xindi Liao, Yongde Zou** and **Baohua Ma:** Conceptualization, Methodology. **Yinbao Wu:** Conceptualization, Writing - review & editing, Project administration, Funding acquisition.

Acknowledgments

This research was funded by the National Key R&D Program of China (2016YFD0501408); the earmarked fund for Modern Agro-industry Technology Research System (CARS-40); WENS Foodstuff Group Co., Ltd, quantification of odor-causing substances in manure fermentation and optimization of their removal methods (YQ20200608FCXY079).

Captions;

Figure 1 Changes of ~~total NH₃ emissions (a) and~~ daily NH₃ emissions (~~b~~) in different treatments.

Figure 2 Changes of Moisture (a), temperature (b), pH (c), EC (d), C/N (e) and TOC (f) in different treatments.

Figure 3 Changes of (TN) total nitrogen (a), NH₄⁺-N (ammonium nitrogen) (b) and NO₃⁻-N (nitrate nitrogen) (c) in different treatments.

Figure 4 The changes in the abundances of total bacteria, ammonia-oxidizing bacteria (AOB) and four kinds of genes during the composting process. (a) total bacteria, (b) AOB, (c) *narG*, (d) *nirK*, (e) *nirS* and (f) *nosZ* gene.

Figure 5 Redundancy analyses of the correlation between the genes, nitrogen emission and physiochemical properties.

Table 1 Main physico-chemical characteristics of the raw materials (dry weight basis): layer manure and sawdust before composting.

Table 2 Main physico-chemical characteristics of the cornstalk biochar (dry weight basis).

Table 3 The primer sequences, expected amplicon size, and annealing temperature for each target gene used in this study.

Table 4 The Brunauer-Emmett-Teller (BET) model results in different treatments.

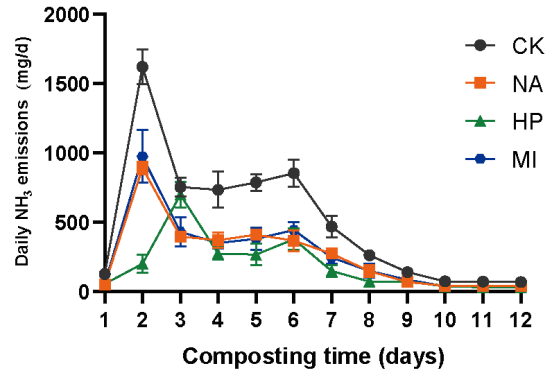


Figure 1 Changes of ~~total NH₃ emissions (a) and~~ daily NH₃ emissions (~~b~~) in different treatments. CK: layer manure +sawdust; NA: layer manure +sawdust +10% HNO₃ biochar; HP: layer manure +sawdust +10% H₂O₂ biochar; MI: layer manure +sawdust +10% HNO₃- H₂O₂ biochar. The bars are presented as standard error. ~~Different letters above columns and symbol of star indicate significant differences ($P < 0.05$) among the four groups.~~

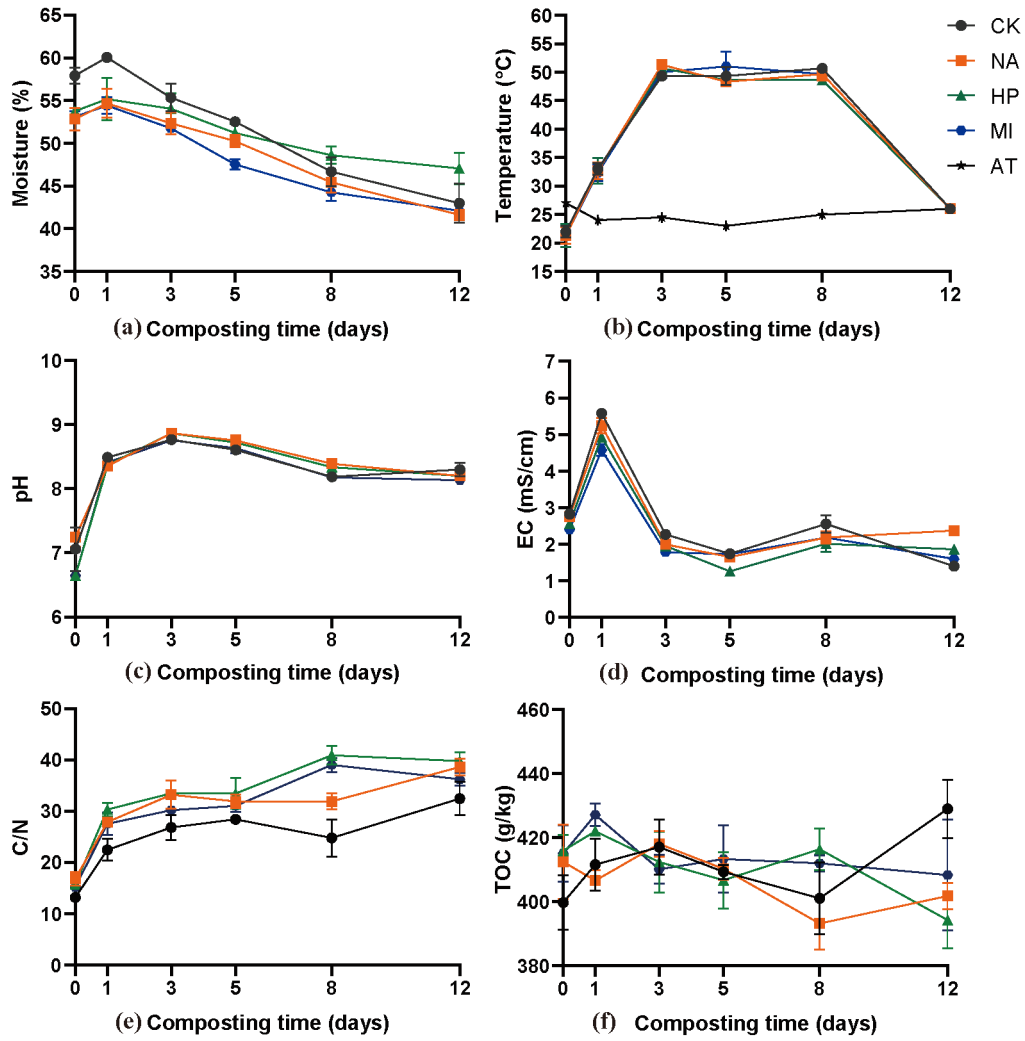


Figure 2 Changes of Moisture (a), temperature (b), pH (c), EC (d), C/N (e) and TOC (f) in different treatments.

CK: layer manure +sawdust; NA: layer manure +sawdust +10% HNO₃ biochar; HP: layer manure +sawdust +10% H₂O₂ biochar; MI: layer manure +sawdust +10% HNO₃- H₂O₂ biochar.

The bars are presented as standard error. TOC-Total Organic Carbon, AT- Ambient Temperature.

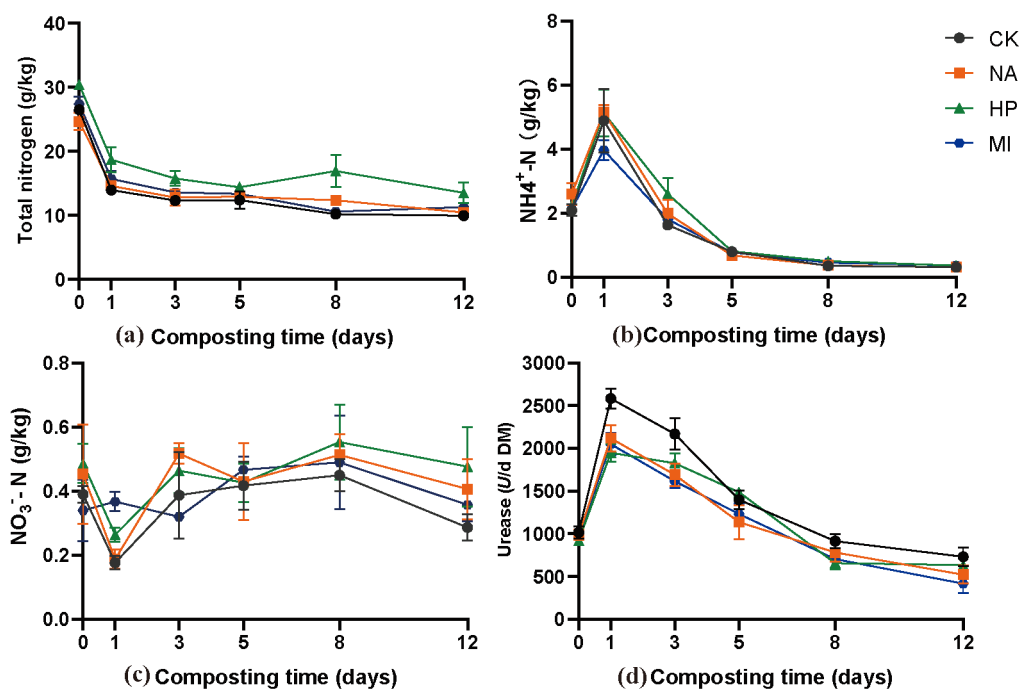


Figure 3 Changes of (TN) total nitrogen (a), $\text{NH}_4^+\text{-N}$ (ammonium nitrogen) (b) and $\text{NO}_3^-\text{-N}$ (nitrate nitrogen) (c) in different treatments.

CK: layer manure +sawdust; NA: layer manure +sawdust +10% HNO_3 biochar; HP: layer manure +sawdust +10% H_2O_2 biochar; MI: layer manure +sawdust +10% HNO_3 - H_2O_2 biochar.

The bars are presented as standard error.

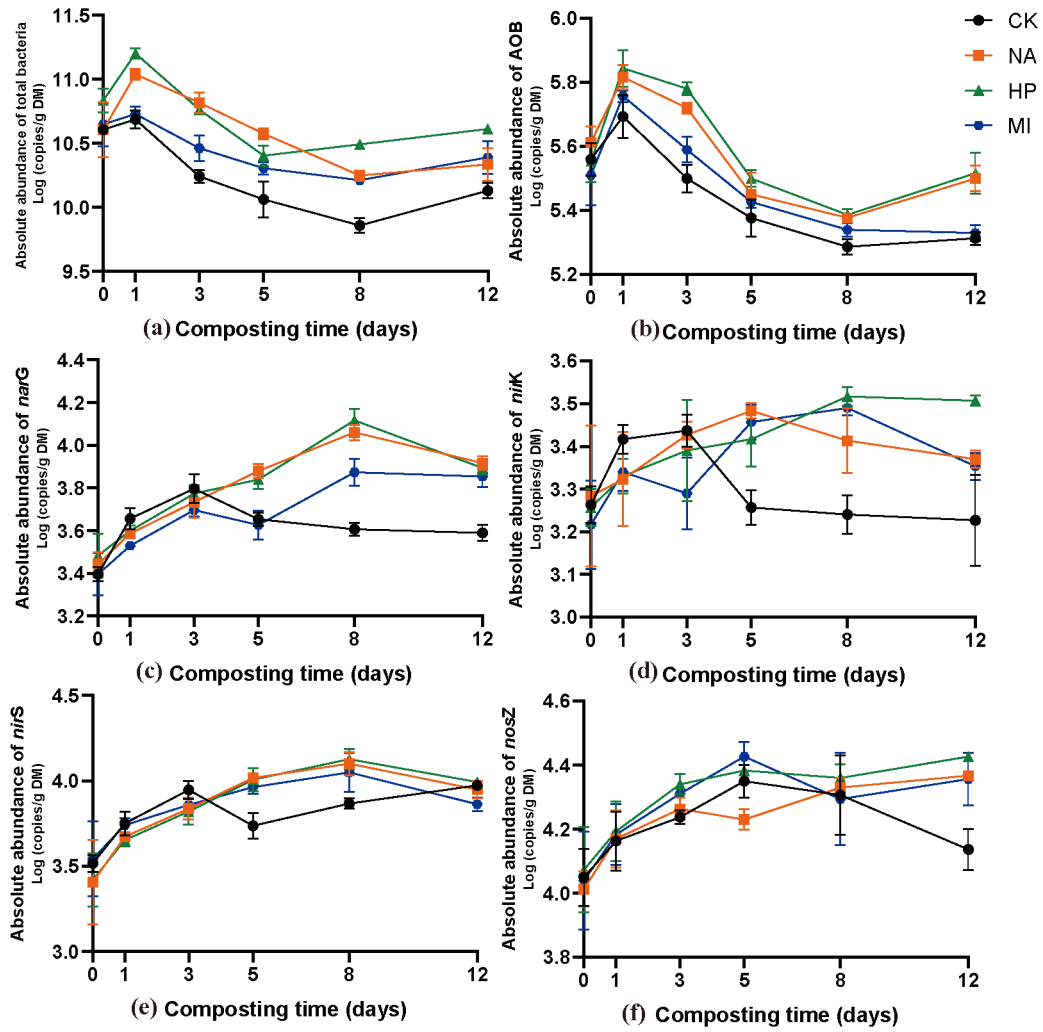


Figure 4 The changes in the abundances of total bacteria, ammonia-oxidizing bacteria (AOB) and four kinds of genes during the composting process. (a) total bacteria, (b) AOB, (c) *narG*, (d) *nirK*, (e) *nirS* and (f) *nosZ* gene.

CK: layer manure +sawdust; NA: layer manure +sawdust +10% HNO_3 biochar; HP: layer manure +sawdust +10% H_2O_2 biochar; MI: layer manure +sawdust +10% HNO_3 - H_2O_2 biochar.

The bars are presented as standard error.

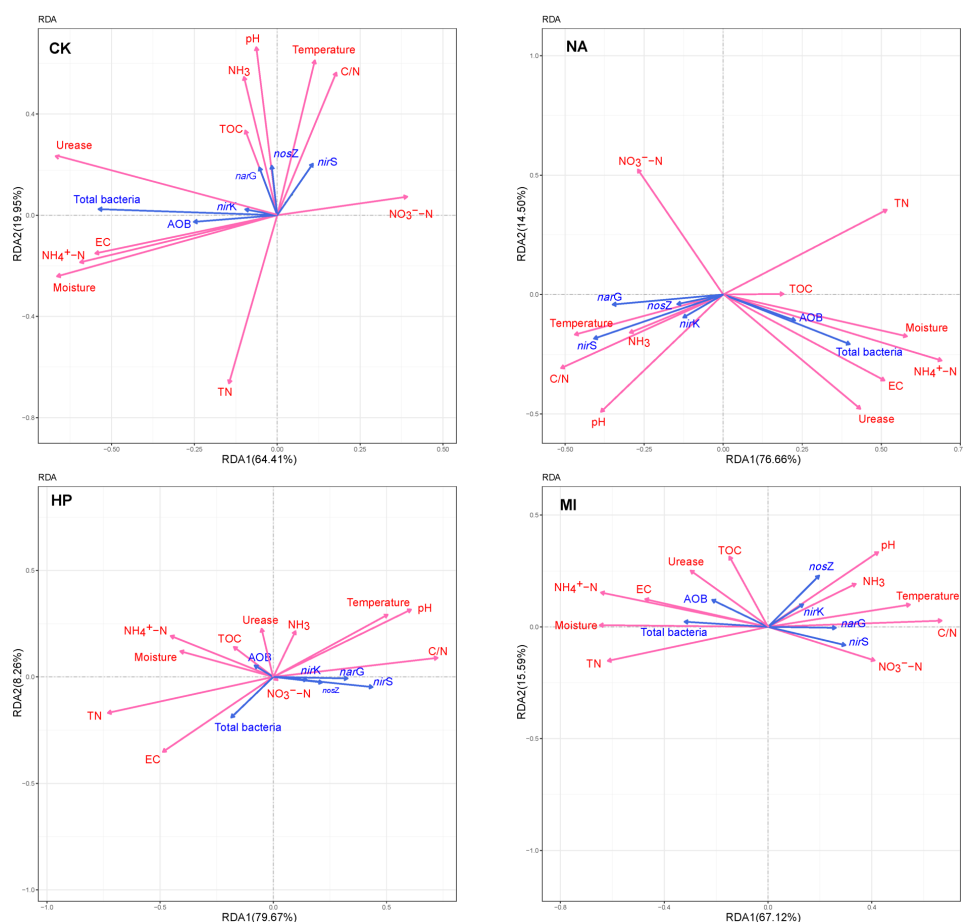


Figure 5 Redundancy analyses of the correlation between the genes, nitrogen emission and physiochemical properties.

CK: layer manure +sawdust; NA: layer manure +sawdust +10% HNO_3 biochar; HP: layer manure +sawdust +10% H_2O_2 biochar; MI: layer manure +sawdust +10% HNO_3 - H_2O_2 biochar.

439 Table 1 Main physico-chemical characteristics of the raw materials (dry weight basis): layer manure and
 440 sawdust before composting.

Parameter	sawdust	Layer manure
Moisture (%)	6.76±0.88	75.40±1.21
TOC g/kg	518.60±2.58	294.20±2.05
TN g/kg	1.08±0.84	68.50±2.23
C/N	483.04±3.85	4.42±0.85

441 TOC-Total Organic Carbon, TN - Total Nitrogen

442

443 Table 2 Main physico-chemical characteristics of the cornstalk biochar (CB) (dry weight basis).

Parameter	CB	HNO ₃ CB	H ₂ O ₂ CB	HNO ₃ - H ₂ O ₂ CB
Moisture (%)	1.02±0.05	1.23±0.10	0.99±0.03	1.21±0.12
TOC g/kg	489.00±56.97	493.67±23.11	481.91±16.80	452.53±30.87
TN g/kg	4.62±0.34	6.70±0.42	4.84±0.44	6.03±0.26
C/N	106.00±10.76	74.00±3.81	100.60±5.80	75.71±8.45

444 CB: cornstalk biochar; HNO₃ CB: 6 mol/L HNO₃ modify CB; H₂O₂ CB: 25% H₂O₂ modify CB; HNO₃-

445 H₂O₂ CB: HNO₃ and H₂O₂ modify CB. TOC-Total Organic Carbon, TN - Total Nitrogen

446

447 Table 3 The primer sequences, expected amplicon size, and annealing temperature for each target
 448 gene used in this study.

Gene name	Primer	Size (bp)	Annealing temperature (°C)	source
<i>AOB-amoA</i>	F: GGGGTT TCTACTGGTGGT R: CCCCTCKGSAAAGCCTTCTTC	491	55	Zhou et al., 2019
<i>narG</i>	F: TAY GTS GGG CAG GAR AAA CTG R: CGT AGA AGA AGC TGG TGG TGT T	483	58	Lópezgutiérrez et al., 2004
<i>nirS</i>	F: GTS AAC GTS AAG GAR ACS GG R: GAS TTC GGR TGS GTC TTG A	425	59	Zhang et al. 2020a
<i>nirK</i>	F: ATCATGGTSC TGCCGCG R: GCCTCGATCAGRTTGTGGTT	471	58	Zhang et al., 2020a
<i>nosZ</i>	F: CGCRACGGCAASAAGGTSMSST R: CAKRTGCAKSGCRTGGCAGAA	268	60	Zhang et al., 2020a
<i>16S V3</i>	F: ATTACCGCGGCTGCTGG R: CCTACGGGAGGCAGCAG	193	55	Zhou et al., 2019

449

450

451 Table 4 The Brunauer-Emmett-Teller (BET) model results in different 4 treatments.

Method	Properties	CB	HNO ₃ CB	H ₂ O ₂ CB	HNO ₃ -H ₂ O ₂ CB
BET	Specific surface area (m ² /g)	255.3158	399.0523	485.4621	405.2281
	Total pore volume (cm ³ /g)	0.1108	0.1479	0.2696	0.1620
	Pore size (nm)	2.1418	2.2182	2.2221	2.3625

452 CB: cornstalk biochar; HNO₃ CB: 6 mol/L HNO₃ modify CB; H₂O₂ CB: 25% H₂O₂ modify CB; HNO₃-

453 H₂O₂ CB: HNO₃ and H₂O₂ modify CB.

454

References

1. Akdeniz, N. 2019. A systematic review of biochar use in animal waste composting. *Waste Manag*, **88**, 291-300.
2. Akiyama, H., Yamamoto, A., Uchida, Y., Hoshino, Y.T., Tago, K., Wang, Y., Hayatsu, M. 2020. Effect of low C/N crop residue input on N₂O, NO, and CH₄ fluxes from Andosol and Fluvisol fields. *Sci Total Environ*, **713**, 10.
3. Awasthi, M.K., Duan, Y.M., Awasthi, S.K., Liu, T., Zhang, Z.Q. 2020. Influence of bamboo biochar on mitigating greenhouse gas emissions and nitrogen loss during poultry manure composting. *Bioresour Technol*, **303**, 10.
4. Awasthi, M.K., Wang, Q., Awasthi, S.K., Wang, M., Chen, H., Ren, X., Zhao, J., Zhang, Z. 2018. Influence of medical stone amendment on gaseous emissions, microbial biomass and abundance of ammonia oxidizing bacteria genes during biosolids composting. *Bioresour Technol*, **247**, 970-979.
5. Chen, H.Y., Awasthi, S.K., Liu, T., Duan, Y.M., Ren, X.N., Zhang, Z.Q., Pandey, A., Awasthi, M.K. 2020a. Effects of microbial culture and chicken manure biochar on compost maturity and greenhouse gas emissions during chicken manure composting. *J Hazard Mater*, **389**, 9.
6. Chen, W., Liao, X., Wu, Y., Liang, J.B., Mi, J., Huang, J., Zhang, H., Wu, Y., Qiao, Z., Li, X., Wang, Y. 2017. Effects of different types of biochar on methane and ammonia mitigation during layer manure composting. *Waste Manag*, **61**, 506-515.
7. Chen, Y., Li, X., Li, S., Xu, Y. 2020b. Effect of C/N ration on disposal of pig carcass by co-composting with swine manure: experiment at laboratory scale. *Environ Technol*, 1-11.
8. De Guardia, A., Petiot, C., Rogeau, D., Druilhe, C. 2008. Influence of aeration rate on nitrogen dynamics during composting. *Waste Manag*, **28**(3), 575-587.
9. Gajalakshmi, S., Abbasi, S. 2008. Solid waste management by composting: state of the art. *Critical Reviews in Environmental Science and Technology*, **38**(5), 311-400.
10. Guo, H., Gu, J., Wang, X., Yu, J., Nasir, M., Zhang, K., Sun, W. 2020a. Microbial driven reduction of N₂O and NH₃ emissions during composting: Effects of bamboo charcoal and bamboo vinegar. *J Hazard Mater*, **390**, 121292.
11. Guo, X.X., Liu, H.T., Zhang, J. 2020b. The role of biochar in organic waste composting and soil improvement: A review. *Waste Manag*, **102**, 884-899.
12. He, X., Yin, H., Han, L., Cui, R., Fang, C., Huang, G. 2019. Effects of biochar size and type on gaseous emissions during pig manure/wheat straw aerobic composting: Insights into multivariate-microscale characterization and microbial mechanism. *Bioresour Technol*, **271**, 375-382.
13. Huang, G.F., Wong, J., Wu, Q., Nagar, B. 2004. Effect of C/N on composting of pig manure with sawdust. *Waste manag*, **24**(8), 805-813.
14. Huff, M.D., Lee, J.W. 2016. Biochar-surface oxygenation with hydrogen peroxide. *J Environ Manag*, **165**, 17-21.
15. Kazak, O., Tor, A. 2020. In situ preparation of magnetic hydrochar by co-hydrothermal treatment of waste vinasse with red mud and its adsorption property for Pb(II) in aqueous solution. *J Hazard Mater*, **393**, 12.
16. Li, F., Cao, X., Zhao, L., Wang, J., Ding, Z. 2014. Effects of mineral additives on biochar formation: carbon retention, stability, and properties. *Environ Sci & Technol*, **48**(19), 11211-11217.
17. Li, H.H., Zhang, T., Tsang, D.C.W., Li, G.X. 2020. Effects of external additives: Biochar, bentonite,

- phosphate, on co-composting for swine manure and corn straw. *Chemosphere*, **248**, 10.
18. Li, Q., Guo, X., Lu, Y., Shan, G., Huang, J. 2016. Impacts of adding FGDG on the abundance of nitrification and denitrification functional genes during dairy manure and sugarcane pressmud co-composting. *Waste Manag*, **56**, 63-70.
 19. Liang, B., Lehmann, J., Solomon, D., Kinyangi, J., Grossman, J., O'Neill, B., Skjemstad, J.O., Thies, J., Luizão, F.J., Petersen, J. 2006. Black carbon increases cation exchange capacity in soils. *Soil Sci Soc Am J*, **70**(5), 1719-1730.
 20. Liang, J., Li, X.M., Yu, Z.G., Zeng, G.M., Luo, Y., Jiang, L.B., Yang, Z.X., Qian, Y.Y., Wu, H.P. 2017. Amorphous MnO₂ Modified Biochar Derived from Aerobically Composted Swine Manure for Adsorption of Pb(II) and Cd(II). *Acs Sustain Chem & Eng*, **5**(6), 5049-5058.
 21. Lin, Y., Munroe, P., Joseph, S., Henderson, R., Ziolkowski, A. 2012. Water extractable organic carbon in untreated and chemical treated biochars. *Chemosphere*, **87**(2), 151-157.
 22. Liu, D., Zhang, R., Wu, H., Xu, D., Tang, Z., Yu, G., Xu, Z., Shen, Q. 2011. Changes in biochemical and microbiological parameters during the period of rapid composting of dairy manure with rice chaff. *Bioresour technol*, **102**(19), 9040-9049.
 23. Liu, N., Zhou, J., Han, L., Ma, S., Sun, X., Huang, G. 2017. Role and multi-scale characterization of bamboo biochar during poultry manure aerobic composting. *Bioresour Technol*, **241**, 190-199.
 24. Liu, T., Kumar Awasthi, M., Kumar Awasthi, S., Duan, Y., Chen, H., Zhang, Z. 2019. Effects of clay on nitrogen cycle related functional genes abundance during chicken manure composting. *Bioresour Technol*, **291**, 121886.
 25. Liu, Y., Ma, R., Li, D., Qi, C., Han, L., Chen, M., Fu, F., Yuan, J., Li, G. 2020. Effects of calcium magnesium phosphate fertilizer, biochar and spent mushroom substrate on compost maturity and gaseous emissions during pig manure composting. *J Environ Manag*, **267**, 110649.
 26. López-Cano, I., Roig, A., Cayuela, M.L., Alburquerque, J.A., Sánchez-Monedero, M.A. 2016. Biochar improves N cycling during composting of olive mill wastes and sheep manure. *Waste Manag*, **49**, 553-559.
 27. Malińska, K., Zabochnicka-Świątek, M., Dach, J. 2014. Effects of biochar amendment on ammonia emission during composting of sewage sludge. *Eco Eng*, **71**, 474-478.
 28. Meng, X.T., Li, Y.Y., Yao, H.Y., Wang, J., Dai, F., Wu, Y.P., Chapman, S. 2020. Nitrification and urease inhibitors improve rice nitrogen uptake and prevent denitrification in alkaline paddy soil. *Appl Soil Ecol*, **154**, 12.
 29. Ren, X.N., Wang, Q., Zhang, Y., Awasthi, M.K., He, Y.F., Li, R.H., Zhang, Z.Q. 2020. Improvement of humification and mechanism of nitrogen transformation during pig manure composting with Black Tourmaline. *Bioresour Technol*, **307**, 10.
 30. Rincon, C.A., De Guardia, A., Couvert, A., Soutrel, I., Guezal, S., Le Serrec, C. 2019. Odor generation patterns during different operational composting stages of anaerobically digested sewage sludge. *Waste Manag*, **95**, 661-673.
 31. Sánchez-García, M., Alburquerque, J.A., Sánchez-Monedero, M.A., Roig, A., Cayuela, M.L. 2015. Biochar accelerates organic matter degradation and enhances N mineralisation during composting of poultry manure without a relevant impact on gas emissions. *Bioresour Technol*, **192**, 272-279.
 32. Sohi, S. 2020. Biochar from Biomass and Waste: Fundamentals and Applications. *Euro J Soil Sci*, **71**(3), 548-549.
 33. Tsui, T.H., Ekama, G.A., Chen, G.H. 2018. Quantitative characterization and analysis of granule

- transformations: Role of intermittent gas sparging in a super high-rate anaerobic system. *Water Res*, **139**, 177-186.
34. Tsui, T.-H., Wong, J.W.C. 2019. A critical review: emerging bioeconomy and waste-to-energy technologies for sustainable municipal solid waste management. *Waste Dispos Sustain Energy*, **1**(3), 151-167.
35. Thomas, C., Idler, C., Ammon, C., Amon, T. 2020. Effects of the C/N ratio and moisture content on the survival of ESBL-producing *Escherichia coli* during chicken manure composting. *Waste Manag*, **105**, 110-118.
36. Wang, Y., Gong, J., Li, J., Xin, Y., Hao, Z., Chen, C., Li, H., Wang, B., Ding, M., Li, W., Zhang, Z., Xu, P., Xu, T., Ding, G.C., Li, J. 2020. Insights into bacterial diversity in compost: Core microbiome and prevalence of potential pathogenic bacteria. *Sci Total Environ*, **718**, 137304.
37. Wei, L., Shutao, W., Jin, Z., Tong, X. 2014. Biochar influences the microbial community structure during tomato stalk composting with chicken manure. *Bioresour technol*, **154**, 148-154.
38. Wu, J., Wei, Z., Zhu, Z., Zhao, Y., Jia, L., Lv, P. 2020. Humus formation driven by ammonia-oxidizing bacteria during mixed materials composting. *Bioresour technol*, **311**, 123500.
39. Xu, Z.C., Li, G.X., Huda, N., Zhang, B.X., Wang, M., Luo, W.H. 2020. Effects of moisture and carbon/nitrogen ratio on gaseous emissions and maturity during direct composting of cornstalks used for filtration of anaerobically digested manure centrate. *Bioresour Technol*, **298**, 9.
40. Xue, Y., Gao, B., Yao, Y., Inyang, M., Zhang, M., Zimmerman, A.R., Ro, K.S. 2012. Hydrogen peroxide modification enhances the ability of biochar (hydrochar) produced from hydrothermal carbonization of peanut hull to remove aqueous heavy metals: batch and column tests. *Chem Eng J*, **200**, 673-680.
41. Yu, H., Xie, B., Khan, R., Yan, H., Shen, G. 2020. The changes in functional marker genes associated with nitrogen biological transformation during organic-inorganic co-composting. *Bioresour Technol*, **295**, 122197.
42. Yu, J., Gu, J., Wang, X.J., Guo, H.H., Wang, J., Lei, L.S., Dai, X.X., Zhao, W.Y. 2020. Effects of inoculation with lignocellulose-degrading microorganisms on nitrogen conversion and denitrifying bacterial community during aerobic composting. *Bioresour Technol*, **313**, 10.
43. Zhang, D., Cui, R., Fu, B., Yang, Y., Wang, P., Mao, Y., Chen, A., Lei, B. 2020a. Shallow groundwater table fluctuations affect bacterial communities and nitrogen functional genes along the soil profile in a vegetable field. *Appl Soil Ecol*, **146**, 103368.
44. Zhang, H., Marchant-Forde, J.N., Zhang, X., Wang, Y. 2020b. Effect of Cornstalk Biochar Immobilized Bacteria on Ammonia Reduction in Laying Hen Manure Composting. *Molecules*, **25**(7).
45. Zhang, J., Lü, F., Shao, L., He, P. 2014. The use of biochar-amended composting to improve the humification and degradation of sewage sludge. *Bioresour technol*, **168**, 252-258.
46. Zhang, L., Zeng, G., Zhang, J., Chen, Y., Yu, M., Lu, L., Li, H., Zhu, Y., Yuan, Y., Huang, A., He, L. 2015. Response of denitrifying genes coding for nitrite (nirK or nirS) and nitrous oxide (nosZ) reductases to different physico-chemical parameters during agricultural waste composting. *Appl Microbiol Biotechnol*, **99**(9), 4059-70.
47. Zhao, S.X., Schmidt, S., Qin, W., Li, J., Li, G.X., Zhang, W.F. 2020. Towards the circular nitrogen economy - A global meta-analysis of composting technologies reveals much potential for mitigating nitrogen losses. *Sci Total Environ*, **704**, 10.
48. Zhou, S., Zhang, X., Liao, X., Wu, Y., Mi, J., Wang, Y. 2019. Effect of Different Proportions of Three

587 Microbial Agents on Ammonia Mitigation during the Composting of Layer Manure. *Molecules*,
588 **24**(13).
589 49. Zhu, L.L., Shen, D.K., Luo, K.H. 2020. A critical review on VOCs adsorption by different porous
590 materials: Species, mechanisms and modification methods. *J Hazard Mater*, **389**, 27.